Inorganica Chimica Acta 394 (2013) 295–299

Contents lists available at SciVerse ScienceDirect

Inorganica Chimica Acta

journal homepage: www.elsevier.com/locate/ica

Note

Phosphorescence of iridium(III) complexes with 2-(2-pyridyl)-1,3,4-oxadiazoles

Nail M. Shavaleev *, Rosario Scopelliti, Michael Grätzel, Mohammad K. Nazeeruddin *

Laboratory of Photonics and Interfaces, École Polytechnique Fédérale de Lausanne, CH-1015 Lausanne, Switzerland

ARTICLE INFO

Article history:
Received 29 April 2012
Received in revised form 23 July 2012
Accepted 27 July 2012
Available online 3 August 2012

Keywords:
Iridium
1,3,4-Oxadiazole
Ligand
Complex
Cyclometalation
Phosphorescence

ABSTRACT

Cationic bis-cyclometalated iridium(III) complexes $[(C^N)_2Ir(N^N)](PF_6)$ with 2-(2′-pyridyl)-5-R-1,3,4-oxadiazoles (N^N; R = 1-adamantyl, mesityl, *N*-diphenylamino) have a redox gap of 2.58–2.68 V and exhibit orange–red phosphorescence in argon-saturated dichloromethane solution with a maximum, quantum yield, and excited-state lifetime of 613–644 nm, 2–6%, and 90–280 ns.

1. Introduction

Tuning of the photophysical properties of phosphorescent cationic iridium(III) complexes $[(C^N)_2Ir(N^N)]^+$ can be achieved by changing the cyclometalating C^N and neutral N^N ligands [1–10]. Here, we report phosphorescent cationic Ir(III) complexes with alkyl, aryl, or diarylamino substituted 2-(2′-pyridyl)-1,3,4-oxadiazoles—a class of easy-to-make neutral N^N ligands rarely used in coordination chemistry (Scheme 1) [11–16]. 1,3,4-Oxadiazole is an electron-deficient heterocycle that finds application as an electron-transport group in organic electronics [17,18]. We note that several research labs recently investigated neutral [19–21] and cationic [22,23] Ir(III) complexes with 1,3,4-oxadiazole-modified cyclometalating ligands.

2. Results and discussion

Three new N^N ligands **L1**–**L3** were prepared by reaction of 5-(2′-pyridyl)-1H-tetrazole with an acyl chloride in pyridine at reflux (Scheme 1) [24]. We chose bulky 1-admantyl (**L1**) and mesityl (**L2**) groups to reduce solid state interaction and to increase solubility of the complexes. We chose a diphenylamino group (**L3**) because it facilitates hole-transport in electroluminescent metal complexes [25]. The reaction of **L1**–**L3** with $[(ppy)_2Ir(\mu\text{-}Cl)]_2$ (ppy = N,$C^{2'}$-2-phenylpyridyl) gave three new Ir(III) complexes $[(ppy)_2Ir(N^N)](PF_6)$, **1**–**3**, after purification by column chromatography on silica (Scheme 1). All new compounds were characterized by elemental analysis, ^1H, ^{13}C, and ^{19}F NMR spectroscopy, and mass-spectrometry.

Fig. 1 shows the X-ray structure of **3**. The Ir(III) ion is in a distorted octahedral $[(C^N)_2Ir(N^N)]^+$ coordination environment. The two nitrogen atoms of the C^N ligands are in trans-position to each other. The Ir–(C^N) bonds are shorter than the Ir–(N^N) ones are (Table 1). The Ir–N (N^N) bond to oxadiazole is shorter than that to pyridine by 0.032 Å (Table 1). The dihedral angles between the rings of the ligands are 6.22° (pyridyl and oxadiazole, N^N) and 1.45° or 13.15° (phenyl and pyridine, C^N). The cations of **3** do not participate in face-to-face π–π stacking, and have the minimum inter-metallic Ir···Ir distance 9.090(2) Å.

Redox potentials of **1**–**3** (relative to Fc^+/Fc [26]) were measured with cyclic voltammetry in acetonitrile and DMF and were found to be solvent-independent (Fig. 2 and Fig. S1, Supporting information). The complexes exhibit a reversible/quasi-reversible reduction of N^N ligand at −1.73 to −1.64 V; an irreversible oxidation of Ir–phenyl fragment at 0.93–0.98 V; and the redox gap, $\Delta E = E^{ox} - E_{1/2}{}^{red}$, 2.58–2.68 V (Table 2). The observed variation of reduction potentials, **3** (−1.73 V) < **1** (−1.68 V) < **2** (−1.64 V), reflects the electron-donor strength of substituents in the N^N ligand: diphenylamino (**3**) > 1-adamantyl (**1**) > mesityl (**2**).

1–**3** exhibit more positive redox potentials than does the reference complex $[(ppy)_2Ir(2,2'\text{-bipyridine})](PF_6)$, −1.77 and 0.84 V in DMF [27] or −1.78 and 0.88 V in acetonitrile [28]; therefore, we conclude that 1,3,4-oxadiazole is a stronger electron-acceptor [17,18] and a weaker σ-electron-donor than is the pyridine.

Ligands **L1**–**L3** are white solids; their electronic absorption spectra exhibit bands at $\lambda < 375$ nm that are enhanced and

* Corresponding authors. Tel.: +41 21 693 6124; fax: +41 21 693 4111.
E-mail addresses: nail.shavaleev@epfl.ch (N.M. Shavaleev), mdkhaja.nazeeruddin@epfl.ch (M.K. Nazeeruddin).

0020-1693/$ - see front matter © 2012 Elsevier B.V. All rights reserved.
http://dx.doi.org/10.1016/j.ica.2012.07.026

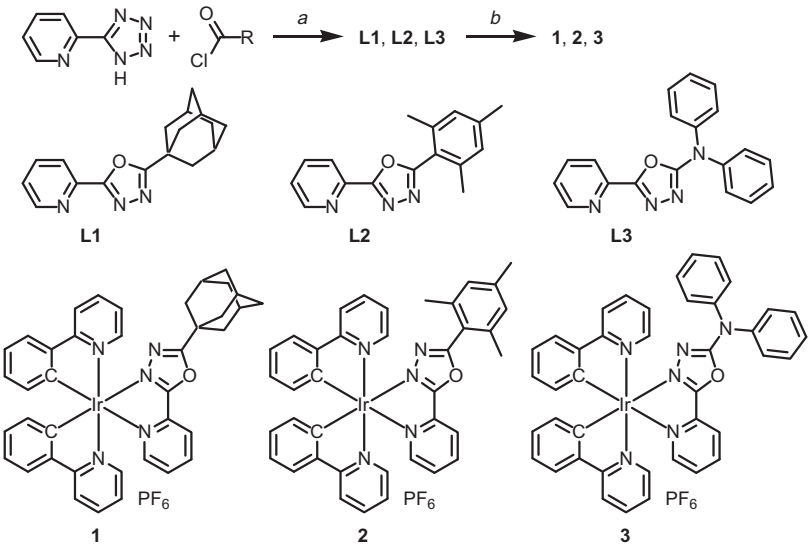

Scheme 1. Synthesis of new ligands and Ir(III) complexes: (a) pyridine, under argon, reflux; (b) $[(C^N)_2Ir(\mu\text{-}Cl)]_2$, under argon, 40 °C, dichloromethane/methanol, KPF_6.

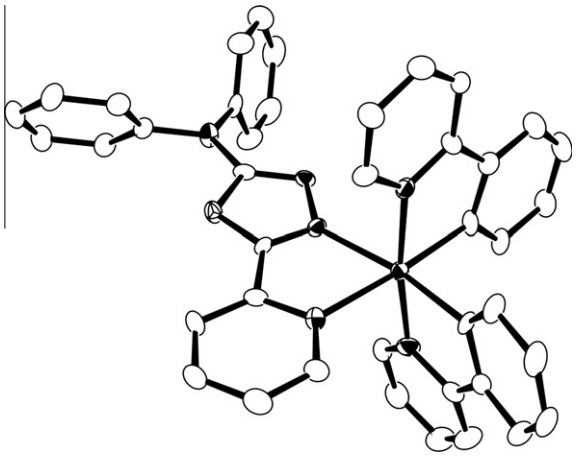

Fig. 1. Structure of **3** (CCDC 878933; 50% probability ellipsoids; H atoms and PF_6 anion are omitted; ORTEP). Heteroatoms are shown as octant ellipsoids: Ir and N, black; O, clear.

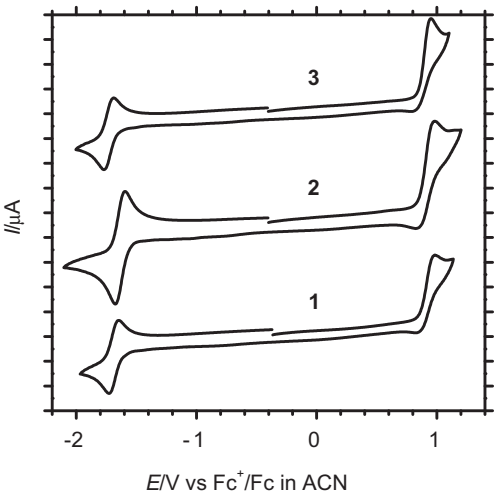

Fig. 2. Cyclic voltammograms of **1**–**3** in acetonitrile (glassy carbon electrode, 0.1 M NBu_4PF_6, 100 mV/s). The unit on the vertical axis is 10 μA. CVs of **1**–**3** in DMF are shown in the Supporting information.

Table 1
Bond lengths (Å) in **3**[a].

C^N		N^N	
Ir–C	Ir–N	Ir–N(py)[b]	Ir–N(oda)[b]
2.000(5)	2.040(6)	2.195(5)	2.163(5)
2.022(6)	2.064(5)		

[a] Each row corresponds to one ligand in the complex.
[b] N(py) and N(oda) are nitrogen atoms of pyridine and 1,3,4-oxadiazole, respectively.

red-shifted when 1-adamantyl group in **L1** is replaced with aromatic (mesityl or diphenylamino) and charge-transfer (diphenylamino-to-oxadiazole) chromophores in **L2** and **L3** (Fig. 3 and Table 3).

The complexes are yellow (**1**) or orange (**2**, **3**) solids; their electronic spectra in dichloromethane (Fig. 4, Table 3, and Fig. S2, Supporting information) display an (Ir–phenyl)-to-(N^N) charge transfer transition at $\lambda > 450$ nm with molar absorption coefficients (ε) of less than 10^3 M^{-1} cm^{-1} [5]. The charge-transfer (MLCT, ILCT)

Table 2
Redox properties[a].

Complex	Solvent	$E_{1/2}^{red}$/V[b]	E^{ox}/V[c]	ΔE/V[d]
1	DMF	−1.68 (98)[e]	0.96	2.64
	ACN	−1.68 (78)	0.98	2.66
2	DMF	−1.64 (88)	0.94	2.58
	ACN	−1.64 (78)	0.98	2.62
3	DMF	−1.73 (83)	0.93	2.66
	ACN	−1.73 (83)	0.95	2.68

[a] In acetonitrile (ACN) or DMF. Relative to Fc^+/Fc. Error: ±50 mV. On glassy carbon working electrode, with 0.1 M $(NBu_4)PF_6$, at scan rate 100 mV/s. The anodic/cathodic peak separation for the standard, Fc^+/Fc couple, was 78–88 mV.
[b] Reversible process (unless stated otherwise). The anodic/cathodic peak separation is given in brackets.
[c] Irreversible process. The return wave was observed in acetonitrile with anodic/cathodic peak separation of more than 150 mV at 100 mV/s. The oxidation peak potential is reported.
[d] $\Delta E = E^{ox} - E_{1/2}^{red}$.
[e] Quasi-reversible process; the anodic/cathodic peak separation is given in brackets.

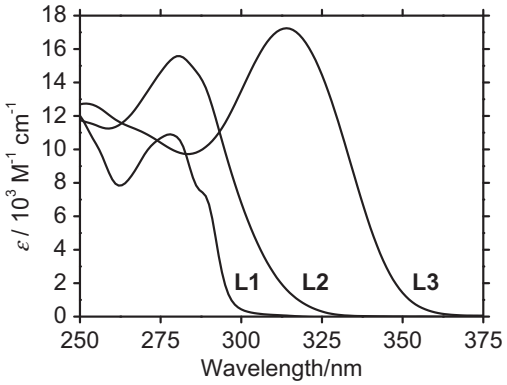

Fig. 3. Absorption spectra of ligands **L1** (2.67×10^{-4} M), **L2** (3.51×10^{-4} M), and **L3** (1.92×10^{-4} M) in dichloromethane.

Table 3
UV–Vis absorption maxima[a].

	λ_{abs}/nm (ε/10^3 M^{-1} cm^{-1})
L1	278 (11), 289 (7.2, sh)
L2	281 (16)
L3	314 (17)
1	269 (46), 359 (7.9), 376 (8.0), 468 (0.8)
2	253 (48), 264 (47), 376 (8.3), 468 (0.8)
3	254 (55), 375 (13, sh), 466 (0.9, sh)

[a] In dichloromethane at room temperature, 250–800 nm. Errors: ±2 nm for λ_{abs}; ±5% for ε.

and ligand π–π* transitions of **1**–**3** are observed at 350–450 nm ($\varepsilon < 13 \times 10^3$ M^{-1} cm^{-1}) and below 350 nm ($\varepsilon < 55 \times 10^3$ M^{-1} cm^{-1}), respectively.

Complexes **1**–**3** in argon-saturated dichloromethane solution exhibit orange–red phosphorescence with a maximum, quantum yield (Φ), and excited-state lifetime (τ) of 613–644 nm, 2–6%, and 90–280 ns (Fig. 5 and Table 4). The excitation spectra of **1**–**3** match the absorption spectra (Fig. S3, Supporting information). The luminescence decays are single exponential functions suggesting the presence of one emissive center in solution (Fig. S4, Supporting information).

The broad emission spectra, the relatively short calculated radiative lifetimes ($\tau_{rad} = \tau/\Phi < 5$ μs), and a direct correlation between the emission energy and the electrochemical gap suggest that **1**–**3** emit from an [(Ir–phenyl)-to-(N^N)] charge-transfer excited state [1,5]. The excited-state deactivation in **1**–**3** is dominated by non-radiative processes, hence $\Phi \leqslant 6\%$ (Table 4). We observe a

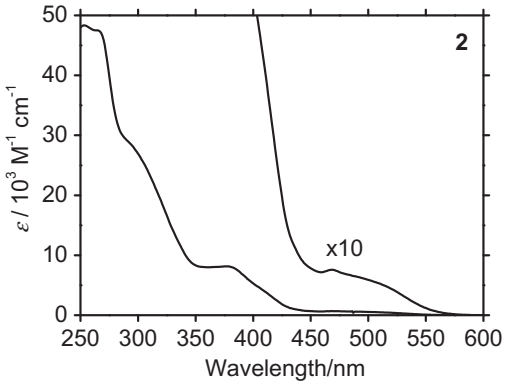

Fig. 4. Absorption spectrum of **2** (6.94×10^{-5} M) in dichloromethane. Additional absorption spectra are shown in the Supporting information.

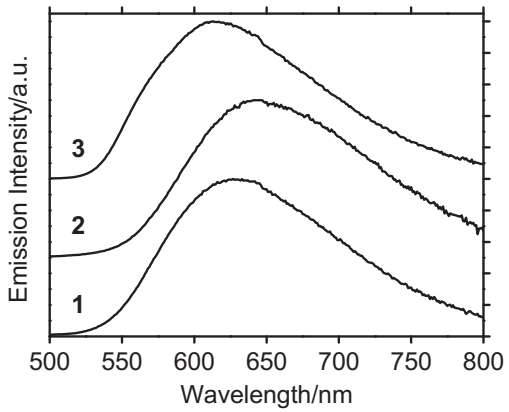

Fig. 5. Corrected and normalized emission spectra of **1**–**3** at 10^{-5} M in argon-saturated dichloromethane at room temperature (λ_{exc} = 350 nm; $\Delta\lambda_{em}$ = 1 nm).

Table 4
Photophysical properties[a].

Complex	λ_{em}/nm	Φ/%	τ/ns	τ_{rad}/μs
1	627	4	170	4
2	644	2	90	5
3	613	6	280	5

[a] In argon-saturated dichloromethane at 10^{-5} M at room temperature. Estimated errors: ±2 nm for λ_{em}; ±20% for Φ and τ_{rad}; ±10 ns for τ.

threefold drop in Φ from **3** to **2** (Table 4), because the contribution of non-radiative processes to the excited state decay increases when the emission energy of Ir(III) complex decreases [5].

The emission maxima of **1**–**3** are red-shifted and the quantum yields are quenched when compared with those of the reference [$(ppy)_2$Ir(2,2′-bipyridine)](PF_6), 585 nm and 14% in acetonitrile [27].

In conclusion, neutral 2-(2′-pyridyl)-1,3,4-oxadiazole ligands, which can be modified in a facile way with functional groups, give phosphorescent cationic bis-cyclometalated Ir(III) complexes. Further tuning of the redox and photophysical properties of these complexes can be achieved by variation of the cyclometalating ligands. We expect 2-(2′-pyridyl)-1,3,4-oxadiazoles to gain wider application in coordination chemistry.

3. Experimental

The following data are provided in the Supporting information: experimental techniques; synthesis of [$(ppy)_2$Ir(μ-Cl)]$_2$; crystallographic data (Table S1); cyclic voltammograms (Fig. S1); absorption spectra (Fig. S2); excitation spectra (Fig. S3); luminescence decays (Fig. S4); ^{1}H, ^{13}C, and ^{19}F NMR spectra.

Purification, crystal growth, and handling of all compounds were carried out under air. All products were stored in the dark. Chemicals from commercial suppliers were used without purification. Chromatography was performed on a column with an i.d. of 30 mm on silica gel 60 (Fluka, Nr 60752). The progress of reactions and the elution of products were followed on TLC plates (silica gel 60 F_{254} on aluminum sheets, Merck).

3.1. Synthesis of the ligands

The structures of **L1**–**L3** are shown in Scheme 1. The reactions were performed under argon. 5-(2′-Pyridyl)-1H-tetrazole (AlfaAesar) was dissolved in pyridine (99.5%, Extra Dry over Molecular Sieves, AcroSeal, Acros). The required acyl chloride was added.

The reaction mixture was stirred at reflux overnight to give pale yellow (**L1**), orange (**L2**), or dark red (**L3**) solution. It was cooled to RT. Further details for the work-up and purification are provided below.

*3.1.1. Ligand **L1***

The reaction was performed with 5-(2′-pyridyl)-1H-tetrazole (500 mg, 3.40 mmol) and 1-adamantanecarboxylic acid chloride (675 mg, 3.40 mmol, Acros) in pyridine (3.5 mL). The reaction mixture was extracted with ether/H_2O. The organic layer was washed with water (to remove pyridine) and evaporated. Purification by column chromatography was performed on silica (10 g). Elution with CH_2Cl_2 removed the impurities. Elution with 0.5% of CH_3OH in CH_2Cl_2 recovered the product. It was re-dissolved in ether, and hexane (20 mL) was added. The ether was rotor-evaporated to leave a suspension of the product in hexane. The suspension was cooled to −15 °C overnight and filtered. The product was washed with cold hexane. The product purified in this way contained 10% of 1-adamantanecarboxylic acid (detected by ^{1}H and ^{13}C NMR). To remove the acid, the product was sonicated in saturated aqueous solution of Na_2CO_3 for 10 min and extracted with ether. The organic layer was washed with saturated aqueous solution of Na_2CO_3 and water. It was evaporated, and the extraction with Na_2CO_3 (aq. sat.) and ether was repeated one more time. White solid: 477 mg (1.70 mmol, 50%). *Anal.* Calc. for $C_{17}H_{19}N_3O$ (MW 281.35): C, 72.57; H, 6.81; N, 14.94. Found: C, 72.54; H, 6.87; N, 14.74%. ^{1}H NMR (400 MHz, [D_6]dmso): δ = 8.79–8.74 (m, 1H), 8.19–8.13 (m, 1H), 8.03 (td, J = 8.0, 1.6 Hz, 1H), 7.62 (ddd, J = 7.6, 4.8, 1.2 Hz, 1H), 2.10–2.04 (m, br, 9H), 1.77 (br, 6H) ppm. ^{13}C NMR (100 MHz, CD_2Cl_2): δ = 173.68, 163.90, 150.34, 144.25, 137.28, 125.72, 123.00, 40.12, 36.44, 34.71, 28.13 ppm. GC–EI$^+$ MS: m/z 281 (M^+, 100%).

*3.1.2. Ligand **L2***

The reaction was performed with 5-(2′-pyridyl)-1H-tetrazole (730 mg, 4.96 mmol) and 2,4,6-trimethylbenzoyl chloride (906 mg, 0.83 mL, 4.96 mmol, AlfaAesar) in pyridine (3.5 mL). The reaction mixture was diluted with water (50 mL) to give suspension. It was stirred for 10 min. The precipitate of the crude product was filtered, washed with water, and extracted with ether/H_2O. The organic layer was washed with water and evaporated. Purification by column chromatography was performed on silica (15 g). Elution with CH_2Cl_2 removed pale yellow impurity. Elution with 0.5% CH_3OH in CH_2Cl_2 recovered the product. White solid: 1.10 g (4.15 mmol, 84%). *Anal.* Calc. for $C_{16}H_{15}N_3O$ (MW 265.31): C, 72.43; H, 5.70; N, 15.84. Found: C, 72.24; H, 5.74; N, 15.53%. ^{1}H NMR (400 MHz, [D_6]dmso): δ = 8.79 (dd, J = 4.8, 0.8 Hz, 1H), 8.24 (dd, J = 8.0, 0.8 Hz, 1H), 8.12–8.04 (m, 1H), 7.69–7.62 (m, 1H), 7.09 (s, 2H), 2.33 (s, 3H), 2.25 (s, 6H) ppm. ^{13}C NMR (100 MHz, CD_2Cl_2): δ = 164.96, 164.51, 150.52, 144.09, 141.48, 138.98, 137.39, 129.06, 125.98, 123.13, 121.19, 21.26, 20.44 ppm. GC–EI$^+$ MS: m/z 265 (M^+, 100%).

*3.1.3. Ligand **L3***

The reaction was performed with 5-(2′-pyridyl)-1H-tetrazole (437 mg, 2.97 mmol) and diphenylcarbamoyl chloride (693 mg, 2.99 mmol, AlfaAesar) in pyridine (3 mL). The reaction mixture on cooling to RT gave suspension. It was diluted with solution of Na_2CO_3 (sat. aq.) and extracted with CH_2Cl_2. The organic layer was washed with water and evaporated. Purification by column chromatography was performed on silica (15 g). Elution with CH_2Cl_2 removed yellow impurity. Elution with 0.5–1.0% CH_3OH in CH_2Cl_2 recovered the product. It was re-dissolved in CH_2Cl_2, and ethanol (20 mL) was added. Dichloromethane was rotor-evaporated to leave a suspension of the product in ethanol. It was cooled to room temperature, filtered, and washed with hexane. White solid: 839 mg (2.67 mmol, 90%). *Anal.* Calc. for $C_{19}H_{14}N_4O$ (MW 314.34): C, 72.60; H, 4.49; N, 17.82. Found: C, 72.66; H, 4.54; N, 17.54%. ^{1}H NMR (400 MHz, [D_6]dmso): δ = 8.66–8.62 (m, 1H), 8.03–7.94 (m, 2H), 7.55–7.51 (m, 1H), 7.50–7.44 (m, 4H), 7.43–7.38 (m, 4H), 7.35–7.29 (m, 2H) ppm. ^{13}C NMR (100 MHz, CD_2Cl_2): δ = 163.34, 159.67, 150.20, 144.03, 142.58, 137.16, 129.79, 126.69, 125.64, 125.24, 122.19 ppm. ESI$^+$ TOF MS: m/z 314 (M^+, 70%).

3.2. Synthesis of the complexes

The structures of **1**–**3** are shown in Scheme 1. The reactions were performed under argon. The solvents were deoxygenated by bubbling with Ar, but they were not dried. [(ppy)$_2$Ir(μ-Cl)]$_2$ (100 mg, 0.093 mmol; Supporting information) and N^N ligand (**L1**, 56 mg; **L2**, 53 mg; **L3**, 60 mg; 0.19–0.20 mmol, small excess) in CH_2Cl_2/CH_3OH (20/4 mL) were stirred overnight at 40 °C to give orange or red solution. It was evaporated. The residue was purified by column chromatography (silica, 15 g). Elution with 2.0–4.0% CH_3OH in CH_2Cl_2 removed the impurities. Elution with 4.0–5.0% CH_3OH in CH_2Cl_2 recovered the product as yellow or orange fractions (these were followed by green/yellow emissive impurities). The desired fractions were evaporated. The product was dissolved in CH_3OH (3 mL), and added drop-wise to a stirred aqueous solution of KPF_6 (390–730 mg, 2.12–3.97 mmol, in 25 mL of water, large excess; Alfa Aesar) in order to convert the complex to the hexafluorophosphate salt. The resulting suspension was stirred for 30 min and filtered. The complex was washed with water, hexane, and ether. **1**–**3** in dichloromethane solution and **2** and **3** in powder exhibit orange–red phosphorescence. **1** exhibits yellow phosphorescence in powder.

*3.2.1. Complex **1***

Yellow solid: 70 mg (0.076 mmol, 41%). *Anal.* Calc. for $C_{39}H_{35}F_6IrN_5OP$ (MW 926.91): C, 50.54; H, 3.81; N, 7.56. Found: C, 50.78; H, 3.92; N, 7.55%. ^{1}H NMR (400 MHz, CD_2Cl_2): δ = 8.37 (d, J = 7.6 Hz, 1H), 8.25 (t, J = 7.6 Hz, 1H), 8.03–7.95 (m, 3H), 7.90–7.82 (m, 3H), 7.74 (d, J = 8.0 Hz, 2H), 7.64 (dd, J = 7.6, 5.2 Hz, 1H), 7.44 (d, J = 5.2 Hz, 1H), 7.18–7.04 (m, 4H), 6.97 (td, J = 7.6, 1.6 Hz, 1H), 6.92 (td, J = 7.6, 1.2 Hz, 1H), 6.31–6.22 (m, 2H), 2.15 (s, br, 9H), 1.90–1.77 (m, 6H) ppm. ^{13}C NMR (100 MHz, CD_2Cl_2): all of the expected signals in the aromatic (29C) and aliphatic (4C) regions were observed, δ = 176.88, 168.42, 167.79, 167.15, 151.66, 150.08, 149.01, 146.41, 144.15, 143.96, 143.92, 141.05, 140.25, 138.50, 138.40, 131.80, 131.42, 130.73, 130.48, 129.97, 125.80, 124.88, 124.47, 123.81, 123.48, 123.28, 122.69, 119.87, 119.73, 39.39, 35.83, 35.58, 27.60 ppm. ^{19}F NMR (376 MHz, CD_2Cl_2): δ = −73.36 (d, J_{P-F} = 710 Hz, PF_6) ppm. ESI$^+$ TOF MS: m/z 782.24 ({M−PF_6}$^+$, 100%).

*3.2.2. Complex **2***

Orange solid: 103 mg (0.113 mmol, 61%). *Anal.* Calc. for $C_{38}H_{31}F_6IrN_5OP$ (MW 910.87): C, 50.11; H, 3.43; N, 7.69. Found: C, 50.35; H, 3.48; N, 7.64%. ^{1}H NMR (400 MHz, CD_2Cl_2): δ = 8.39 (d, J = 7.6 Hz, 1H), 8.27 (t, J = 7.6 Hz, 1H), 8.07–7.97 (m, 4H), 7.92–7.83 (m, 2H), 7.79 (dd, J = 8.0, 1.2 Hz, 1H), 7.73 (dd, J = 7.6, 1.2 Hz, 1H), 7.71–7.64 (m, 1H), 7.51 (d, J = 5.2 Hz, 1H), 7.19–7.02 (m, 4H), 7.05 (s, 2H), 7.00 (td, J = 7.6, 1.2 Hz, 1H), 6.92 (td, J = 7.6, 1.2 Hz, 1H), 6.39 (dd, J = 7.6, 0.8 Hz, 1H), 6.32 (dd, J = 8.0, 0.8 Hz, 1H), 2.37 (s, 3H), 2.23 (s, 6H) ppm. ^{13}C NMR (100 MHz, CD_2Cl_2): only 31C out of the expected 33C signals were observed in the aromatic region; the expected 2C signals were observed in the aliphatic region; δ = 169.05, 168.05, 167.80, 167.28, 151.79, 150.02, 148.81, 146.72, 143.98, 143.85, 143.25, 140.87, 140.35, 139.21, 138.57, 138.51, 131.82, 130.74, 130.69, 130.03, 129.35, 126.13, 124.96, 124.46, 123.78, 123.56, 123.30, 122.80, 119.97, 119.63,

118.12, 21.15 (CH_3), 20.24 (CH_3) ppm. ^{19}F NMR (376 MHz, CD_2Cl_2): $\delta = -73.33$ (d, $J_{P-F} = 710$ Hz, PF_6) ppm. ESI$^+$ TOF MS: m/z 766.20 ($\{M-PF_6\}^+$, 100%).

3.2.3. Complex **3**

Orange solid: 124 mg (0.129 mmol, 69%). *Anal.* Calc. for $C_{41}H_{30}F_6IrN_6OP$ (MW 959.90): C, 51.30; H, 3.15; N, 8.76. Found: C, 51.26; H, 3.16; N, 8.58%. ^1H NMR (400 MHz, CD_2Cl_2): $\delta = 8.16$ (d, $J = 5.2$ Hz, 1H), 8.08 (t, $J = 7.2$ Hz, 1H), 8.03–7.92 (m, 3H), 7.92–7.84 (m, 3H), 7.76–7.68 (m, 2H), 7.54–7.43 (m, 6H), 7.43–7.35 (m, 6H), 7.27–7.20 (m, 1H), 7.15–7.07 (m, 2H), 7.02 (td, $J = 7.6$, 0.8 Hz, 1H), 6.96 (td, $J = 7.6$, 1.6 Hz, 1H), 6.88 (td, $J = 7.6$, 1.2 Hz, 1H), 6.28–6.22 (m, 2H) ppm. ^{13}C NMR (100 MHz, CD_2Cl_2): only 32C out of the expected 33C signals were observed in the aromatic region, $\delta = 167.87$, 166.96, 164.14, 162.94, 151.36, 150.60, 149.00, 146.60, 144.42, 144.02, 143.73, 141.28, 140.68, 139.84, 138.41, 138.34, 131.71, 131.43, 130.61, 129.94, 129.15, 128.02, 125.93, 124.79, 124.40, 124.07, 123.96, 123.43, 123.16, 122.63, 119.72, 119.67 ppm. ^{19}F NMR (376 MHz, CD_2Cl_2): $\delta = -73.33$ (d, $J_{P-F} = 710$ Hz, PF_6) ppm. ESI$^+$ TOF MS: m/z 815.2 ($\{M-PF_6\}^+$, 100%).

Acknowledgment

European Union (CELLO, STRP 248043; http://www.cello-project.eu/).

Appendix A. Supplementary material

CCDC 878933 contains the supplementary crystallographic data for complex **3**. These data can be obtained free of charge from The Cambridge Crystallographic Data Centre via www.ccdc.cam.ac.uk/data_request/cif. Supplementary data associated with this article can be found, in the online version, at http://dx.doi.org/10.1016/j.ica.2012.07.026.

References

[1] L. Flamigni, A. Barbieri, C. Sabatini, B. Ventura, F. Barigelletti, Top. Curr. Chem. 281 (2007) 143.
[2] C. Ulbricht, B. Beyer, C. Friebe, A. Winter, U.S. Schubert, Adv. Mater. 21 (2009) 4418.
[3] T. Hu, L. He, L. Duan, Y. Qiu, J. Mater. Chem. 22 (2012) 4206.
[4] M.S. Lowry, W.R. Hudson, R.A. Pascal Jr., S. Bernhard, J. Am. Chem. Soc. 126 (2004) 14129.
[5] A.B. Tamayo, S. Garon, T. Sajoto, P.I. Djurovich, I.M. Tsyba, R. Bau, M.E. Thompson, Inorg. Chem. 44 (2005) 8723.
[6] Q. Zhao, S. Liu, M. Shi, C. Wang, M. Yu, L. Li, F. Li, T. Yi, C. Huang, Inorg. Chem. 45 (2006) 6152.
[7] M. Mydlak, C. Bizzarri, D. Hartmann, W. Sarfert, G. Schmid, L. De Cola, Adv. Funct. Mater. 20 (2010) 1812.
[8] S. Ladouceur, D. Fortin, E. Zysman-Colman, Inorg. Chem. 49 (2010) 5625.
[9] V. Aubert, L. Ordronneau, M. Escadeillas, J.A.G. Williams, A. Boucekkine, E. Coulaud, C. Dragonetti, S. Righetto, D. Roberto, R. Ugo, A. Valore, A. Singh, J. Zyss, I. Ledoux-Rak, H. Le Bozec, V. Guerchais, Inorg. Chem. 50 (2011) 5027.
[10] D. Sykes, I.S. Tidmarsh, A. Barbieri, I.V. Sazanovich, J.A. Weinstein, M.D. Ward, Inorg. Chem. 50 (2011) 11323.
[11] J.P. Wignacourt, S. Sueur, M. Lagrenée, Acta Crystallogr., Sect. C 46 (1990) 394.
[12] A. Gueddi, B. Mernari, M. Giorgi, M. Pierrot, Acta Crystallogr., Sect. C 56 (2000) E426.
[13] V.J. Catalano, T.J. Craig, Inorg. Chem. 42 (2003) 321.
[14] Y.-T. Wang, M.-L. Tong, H.-H. Fan, H.-Z. Wang, X.-M. Chen, Dalton Trans. (2005) 424.
[15] F. Wei, L. Fang, Y. Huang, Inorg. Chim. Acta 363 (2010) 2600.
[16] L.-F. Shi, Y. Li, Z. Si, Y. Guan, H. Cao, Acta Crystallogr., Sect. E 67 (2011) m9.
[17] A.P. Kulkarni, C.J. Tonzola, A. Babel, S.A. Jenekhe, Chem. Mater. 16 (2004) 4556.
[18] G. Hughes, M.R. Bryce, J. Mater. Chem. 15 (2005) 94.
[19] L. Chen, C. Yang, J. Qin, J. Gao, H. You, D. Ma, J. Organomet. Chem. 691 (2006) 3519.
[20] Z. Xu, Y. Li, X. Ma, X. Gao, H. Tian, Tetrahedron 64 (2008) 1860.
[21] Y. Zheng, A.S. Batsanov, M.R. Bryce, Inorg. Chem. 50 (2011) 3354.
[22] G.-G. Shan, D.-X. Zhu, H.-B. Li, P. Li, Z.-M. Su, Y. Liao, Dalton Trans. 40 (2011) 2947.
[23] F. Gärtner, S. Denurra, S. Losse, A. Neubauer, A. Boddien, A. Gopinathan, A. Spannenberg, H. Junge, S. Lochbrunner, M. Blug, S. Hoch, J. Busse, S. Gladiali, M. Beller, Chem. Eur. J. 18 (2012) 3220.
[24] R. Huisgen, J. Sauer, H.J. Sturm, Angew. Chem. 70 (1958) 272.
[25] G. Zhou, W.-Y. Wong, X. Yang, Chem. Asian J. 6 (2011) 1706.
[26] R.R. Gagné, C.A. Koval, G.C. Lisensky, Inorg. Chem. 19 (1980) 2854.
[27] R.D. Costa, E. Ortí, D. Tordera, A. Pertegás, H.J. Bolink, S. Graber, C.E. Housecroft, L. Sachno, M. Neuburger, E.C. Constable, Adv. Energy Mater. 1 (2011) 282.
[28] F.O. Garces, K.A. King, R.J. Watts, Inorg. Chem. 27 (1988) 3464.